Aeolian iron input to the ocean through precipitation scavenging: A modeling perspective and its implication for natural iron fertilization in the ocean

Yuan Gao,[1] Song-Miao Fan, and Jorge L. Sarmiento

Program in Atmospheric and Oceanic Sciences, Princeton University, Princeton, New Jersey, USA

Received 5 April 2002; revised 15 August 2002; accepted 9 December 2002; published 12 April 2003.

[1] Aeolian dust input may be a critical source of dissolved iron for phytoplankton growth in some oceanic regions. We used an atmospheric general circulation model (GCM) to simulate dust transport and removal by dry and wet deposition. Model results show extremely low dust concentrations over the equatorial Pacific and Southern Ocean. We find that wet deposition through precipitation scavenging accounts for ~40% of the total deposition over the coastal oceans and ~60% over the open ocean. Our estimates suggest that the annual input of dissolved Fe by precipitation scavenging ranges from 0.5 to 4 $\times$ 10^{12} g yr^{-1}, which is 4–30% of the total aeolian Fe fluxes. Dissolved Fe input through dry deposition is significantly lower than that by wet deposition, accounting for only 0.6–2.4 % of the total Fe deposition. Our upper limit estimate on the fraction of dissolved Fe in the total atmospheric deposition is thus more than three times higher than the value of 10% currently considered as an upper limit for dissolved Fe in Aeolian fluxes. As iron input through precipitation may promote episodic phytoplankton growth in the ocean, measurements of dissolved iron in rainwater over the oceans are needed for the study of oceanic biogeochemical cycles. *INDEX TERMS:* 0312 Atmospheric Composition and Structure: Air/sea constituent fluxes (3339, 4504); 1615 Global Change: Biogeochemical processes (4805); 3210 Mathematical Geophysics: Modeling; 4875 Oceanography: Biological and Chemical: Trace elements; *KEYWORDS:* Aeolian iron, dust modeling, wet and dry deposition, iron fertilization, precipitation

Citation: Gao, Y., S.-M. Fan, and J. L. Sarmiento, Aeolian iron input to the ocean through precipitation scavenging: A modeling perspective and its implication for natural iron fertilization in the ocean, *J. Geophys. Res.*, *108*(D7), 4221, doi:10.1029/2002JD002420, 2003.

1. Introduction

[2] Recent iron (Fe) fertilization experiments conducted in the equatorial Pacific [*Martin et al.*, 1994; *Coale et al.*, 1996a] and Southern Ocean [*Boyd et al.*, 2000] provide strong evidence to support the hypothesis that Fe, a micronutrient, plays an important role in regulating phytoplankton growth in the ocean. These results also suggest that Fe fertilization may affect the cycles of other nutrients in the ocean, especially nitrogen [*Capone et al.*, 1997; *Falkowski*, 1997]. Consequently the input of Fe to the ocean may affect the ocean carbon cycle and thus atmospheric carbon dioxide and global climate both at present and in the past [*Martin*, 1990; *Broecker and Henderson*, 1998; *Petit et al.*, 1999; *Watson and Lefevre*, 1999]. Therefore, understanding the supply and cycles of Fe in the ocean is critically important [*Fung et al.*, 2000; *Archer and Johnson*, 2000].

[3] The major source of Fe in the surface waters of certain open ocean regions is aeolian dust deposition [*Duce and Tindale*, 1991], although evidence of the relative importance of this versus in situ iron supply by upwelling waters from below is mixed [*Coale et al.*, 1996a]. Recent calculations suggest that the total deposition of aeolian Fe to the global ocean is about 14 $\times$ 10^{12} g yr^{-1}, with the distribution varying strongly with season and from one ocean region to another [*Gao et al.*, 2001]. The major processes that control the delivery of aeolian Fe to the ocean are dry deposition by particle gravitational settling and turbulence in the surface layer of the atmosphere, and wet deposition through precipitation scavenging [*Jickells and Spokes*, 2001]. During long-range transport, dust particles may undergo heterogeneous reactions at gas-solid-liquid interfaces [*Underwood et al.*, 2001; *Dentener et al.*, 1996]. Photochemical reduction in more acidic cloud waters and precipitation may promote dissolution of Fe in dust, leading to the production of soluble Fe (II), which is believed to be more readily used by phytoplankton [*Sunda*, 2001]. As biological uptake of Fe largely depends on its solubility and chemical speciation in seawater [*Wells et al.*, 1995], wet deposition through precipitation could be more efficient than dry deposition in

[1] Also at Institute of Marine and Coastal Sciences, Rutgers University, New Brunswick, New Jersey, USA.

0148-0227/03/2002JD002420$09.00

delivering bio-avaliable Fe to the ocean to promote biological responses. An evaluation of the relative contributions of aeolian Fe input by wet deposition in comparison with dry deposition will improve our understanding of the controls on primary productivity in the surface oceans.

[4] In this study, we use an atmospheric general circulation model (GCM) to simulate the transport and deposition of dust and to evaluate the relative contributions of dry and wet deposition in delivering Fe to the ocean. We also use aerosol data obtained from in situ measurements at 73 marine locations to derive Fe deposition to compare with the GCM model results. The transport model and dust simulations are described in section 2. Model results are described in section 3, with an evaluation by comparison to observations. The significance of dissolved iron in rainwater to marine biology is discussed in section 4. We hope that our preliminary results from this work may encourage more detailed characterization of aeolian Fe fertilization in the ocean. In particular, the episodic nature of the aeolian Fe input through precipitation scavenging deserves more attention.

2. Method

2.1. GCM Model Simulations

[5] The Geophysical Fluid Dynamics Laboratory (GFDL) SKYHI general circulation model [*Mahlman et al.*, 1994] was used to simulate dust transport in this study. The SKYHI model has 10 terrain following levels with standard heights of 0.08, 0.27, 0.74, 1.38, 2.16, 3.07, 4.10, 5.23, 6.45, 7.75 km, and 30 pressure levels with nominal standard heights of 9.12, 10.55, 12.01, 13.46, 14.89, etc. up to 80 km. The model has a horizontal grid size of $3^\circ \times 3.6^\circ$ latitude by longitude and a time step of 225 seconds. Short- and long-wave radiation are updated every 4 hours. The model specifies climatological surface albedo, cloud cover, and sea surface temperature. The model uses a nonlocal parameterization for vertical mixing in the planetary boundary layer [*Holtslag and Boville*, 1993]. After each advection time step, a dry or moist convective adjustment is done for potential temperature (but not for dust mixing ratios) when the air column is unstable, and then precipitation rate is calculated. The geographical distribution of the annual-mean and seasonal precipitation in SKYHI was previously compared with observations and was found to be reasonably well simulated [*Hamilton et al.*, 1995].

[6] Dust is transported in the model by integrating the following continuity equation [*Mahlman and Moxim*, 1978; *Levy and Moxim*, 1987]:

$$d(Rp)/dt = \text{ADVECTION} + \text{DIFFUSION} + \text{SOURCE} - DRp - WRp \quad (1)$$

where R is the mass mixing ratio of dust (g g^{-1}), p is the surface pressure (dyn cm^{-2}), D is the dry deposition coefficient (s^{-1}), W is the precipitation removal rate (s^{-1}), and SOURCE includes the surface emission in the bottom layer. Gravitational settling moves dust from the upper layer (negative SOURCE) to lower layer (positive SOURCE). The model was initiated with a uniform distribution of dust. The simulations were carried out for one year, after six months of spin-up.

Table 1. Dust Parameterization in the GFDL SKYHI GCM

Size Bin, μm	Effective Radius, μm	Settling Velocity, cm s^{-1}	Dry Deposition Velocity,[a] cm s^{-1}
GISS			
<1	0.73	0.018	0.2
1–10	6.2	1.2	1.0
GOCART			
<1	0.77	0.02	0.2
1–2	1.5	0.08	1.0
2–3	2.5	0.2	1.0
3–6	4.5	0.7	1.0

[a]Sensitivity test on two pairs of dry deposition velocities, 1 or 3 cm s^{-1} for silt and 0.2 or 0.6 cm s^{-1} for clay, indicates that a dry deposition velocity of 1 cm s^{-1} for silt and 0.2 cm s^{-1} for clay fits better with observations.

[7] We used two dust sources in our model simulations. The first is taken from the Goddard Institute for Space Studies (GISS) [*Tegen and Fung*, 1994]. The GISS monthly emission fields have two size bins of dust particles, 0.1–1 μm (clay) and 1–10 μm (silt). The second dust source is from the Georgia Tech/Goddard Global Ozone Chemistry Aerosol Radiation and Transport (GOCART) model [*Ginoux et al.*, 2001], which was used for comparison. The GOCART source considers dust emissions from dry lakebeds, which represents a new approach in identifying potential dust sources. Monthly dust emissions are given in four size bins in the GOCART, <1 μm, 1–2 μm, 2–3 μm, and 3–6 μm. The different size bins are transported separately in the model.

[8] Gravitational settling velocities were calculated based on Stokes Law, as discussed by *Genthon* [1992] and *Tegen and Fung* [1994]. Settling velocities for different size bins are shown in Table 1. For example, on the basis of Tegen and Fung's calculations, a gravitational settling velocity of 1.2 cm s^{-1} is used to represent silt particles (1–10 μm) corresponding to a mean effective radius of 6.2 μm. For clay particles (<1 μm), a gravitational settling velocity of 0.018 cm s^{-1} is used corresponding to a mean effective radius of 0.73 μm.

[9] Dry deposition is parameterized in SKYHI as "resistances in series," that is, the total resistance to dry deposition is the sum of aerodynamic resistance (reflecting surface layer eddies, inversely related to the surface friction velocity) and surface resistance (inversely related to the dry deposition velocity) [*Hicks et al.*, 1987; *Balkanski et al.*, 1993]. The surface dry deposition velocity is calculated as the inverse of the sum of the resistances. The dry deposition coefficient (D) in equation (1) is then the velocity divided by the thickness of the bottom layer of the atmosphere. The silt particles are assigned a surface dry deposition velocity of 1 or 3 cm s^{-1} (two values were used for a sensitivity test). The clay particles are assigned a surface dry deposition velocity of 0.2 or 0.6 cm s^{-1}. Results of sensitivity tests indicate that a surface dry deposition velocity of 1 cm s^{-1} for silt and 0.2 cm s^{-1} for clay particles fit better with observations. These values will be used in the following discussions.

[10] Wet removal of dust is assumed proportional to the rate of precipitation during the time step of model integration, parameterized as by *Balkanski et al.* [1993]. The Balkanski parameterization was adapted from *Giorgi and Chameides* [1986] for in-cloud scavenging and from *Dana and Hales*

[1976] for below-cloud scavenging. This parameterization resulted in too fast a removal of dust in SKYHI as indicated by comparisons of modeled concentrations with observations (see section 3). Recently, *Cooke et al.* [2002] simulated carbonaceous aerosols in SKYHI using the Balkanski parameterization and also found that the wet removal of carbonaceous aerosols was too fast. They compared model simulations and observations of the accumulative probability of precipitation events from low (0.01 cm day^{-1}) to high rates (10 cm day^{-1}), and found that no rain and light rain events (< 0.1 cm day^{-1}) accounted for 60–70% of the time in both model and observations. However, light rain occurs more frequently in SKYHI than in the observations. In our dust simulations, we chose to use a range of threshold precipitation rates, above which wet removal is activated, instead of tuning a single scavenging ratio as by *Tegen and Fung* [1994]. We tested threshold precipitation rates of 0.01, 0.1, and 1 cm day^{-1} to determine the different effects on wet removal. We found that threshold precipitation rates of 0.01 and 0.1 cm day^{-1} produce similar wet deposition. However, threshold rates between 0.1 and 1 cm day^{-1} result in significant differences in wet deposition. A threshold rate of 1 cm day^{-1} fits better with dust observations, so this is the value we used for the simulations discussed here. We will show a comparison of two scenarios with threshold rates of 0.01 and 1 cm day^{-1} respectively in section 3.

[11] We assume that Fe accounts for 3.5% of the total dust mass, based on the mean crustal composition of *Taylor and McLennan* [1985] and measurements of *Zhu et al.* [1997]. We should mention that although the assumption of 3.5% Fe in dust has been widely used, the exact content of Fe in dust does vary from different source regions [*Claquin et al.*, 1999]. As discussed by *Sokolik and Toon* [1999], dust from the Sahelian region has a high Fe/Al ratio attributed to the abundance of ferrous soils in that region. Dust from semi-arid regions in central Asia, however, contains less Fe than the mean. For example, the average content of Fe in Chinese loess is 3.1% [*GSS*, 1984]. The abundance of Fe in soils and rocks for large areas of continental crust averages from 2.9 to 4.8% [*Tayle and McClennan*, 1985]. Therefore the spatial variation in Fe content will add uncertainty to the estimate of aeolian Fe deposition fluxes. As many investigators have used 3.5% as an average value for the Fe content in dust in their studies, we decided to use the same value for the purpose of comparison.

2.2. Deposition Calculation Based on Dust Measurements

[12] We compare the SKYHI results to in situ dust data obtained from 73 marine locations [*Gao et al.*, 2001], which have been analyzed using simple dry and wet deposition models such as those of *Duce and Tindale* [1991] and *Jickells and Spokes* [2001] to calculate the dry and wet deposition at each location. In these models, the dry deposition flux of Fe is calculated as the product of measured air concentrations of Fe and a dry deposition velocity. We partition the measured total concentrations into two groups, a fine-size group accounting for 80% of the total mass and a coarse-size group accounting for 20% of the total mass, based on measurement results of *Arimoto et al.* [1997], *Gao et al.* [1997], and *Perry and Cahill* [1999], who characterized the size distributions of dust particles in the marine atmosphere. We then apply dry deposition velocities of 0.25 cm s^{-1} to the fine particle group and 1.1 cm s^{-1} to the coarse particle group [*Arimoto et al.*, 1997]. This parameterization is supported by studies using sediment trap measurements in the ocean. Jickells and colleagues [*Jickells*, 1999; *Jickells and Spokes*, 2001] estimated dust flux to a 3000-m depth sediment trap in the Sargasso Sea where the lateral oceanic fluxes are not significant, and they derived a dry deposition velocity of 1.0 cm s^{-1} at this location, which is consistent with dust deposition estimates by *Prospero* [1996a]. The wet removal of Fe via precipitation is estimated using an updated scavenging ratio of 200 [*Jickells and Spokes*, 2001]. The scavenging ratio relates the Fe concentration in dust with that in precipitation [*Jickells and Spokes*, 2001]. The continued use of this approach is due largely to the fact that simultaneous measurements of Fe in dust and in precipitation are sparse. We note that dust flux estimates based on marine boundary layer measurements may not be accurate, since dust concentrations at cloud height and at surface level could be different, and thus these estimates involve substantial uncertainties. Monthly precipitation rates were derived from the global precipitation climatology of *da Silva et al.* [1994].

3. Dust Concentrations

[13] We focus initially on the Asian-Pacific region where more dust measurement data are available for comparison with the model. We examine how the atmospheric Fe concentration varies as a function of distance from the Asian continent (Figure 1). We present a comparison of two model scenarios: standard removal at a threshold precipitation rate of 0.01 cm day^{-1} for wet deposition, and reduced removal at a threshold precipitation rate of 1 cm day^{-1}. We choose the SKYHI modeled concentrations along the 36°N latitudinal line at 10 degree intervals from the Asian coast to the North Pacific (120°–220°), which is within the path of Asian dust transport [*Uematsu et al.*, 1983]. The in situ measurement data obtained at locations within the 26°–46°N band are compared to the modeled concentrations. The comparison suggests that the wet removal calculated with a threshold precipitation rate of 1 cm day^{-1} results in a better fit with observations.

[14] Figure 2 shows that, as would be expected, the clay fraction simulated in SKYHI becomes more and more dominant downwind of the sources from Asia, reflecting a shift toward smaller particles of dust mass-size distribution with increasing distance from the source regions. However, after transport distances of several thousand kilometers, the dust size distributions tend to stabilize, which is consistent with observations [*Arnold et al.*, 1998; *Arimoto et al.*, 1997; *Prospero*, 1996b]. In addition to dust measurement data, results from deep-sea sediment studies conducted in a broad region of the North Pacific reveal that the median grain sizes for the mineral fraction of the sediments change little over the open ocean [*Rea and Hovan*, 1995]. This suggests that dust input to the ocean is dominated by dust particles with a distribution of relatively small grain size. The importance of fine particles is that they may have high Fe content. A recent study in the Arabian Sea by *Siefert et al.* [1999] found that soluble Fe (II) was primarily released

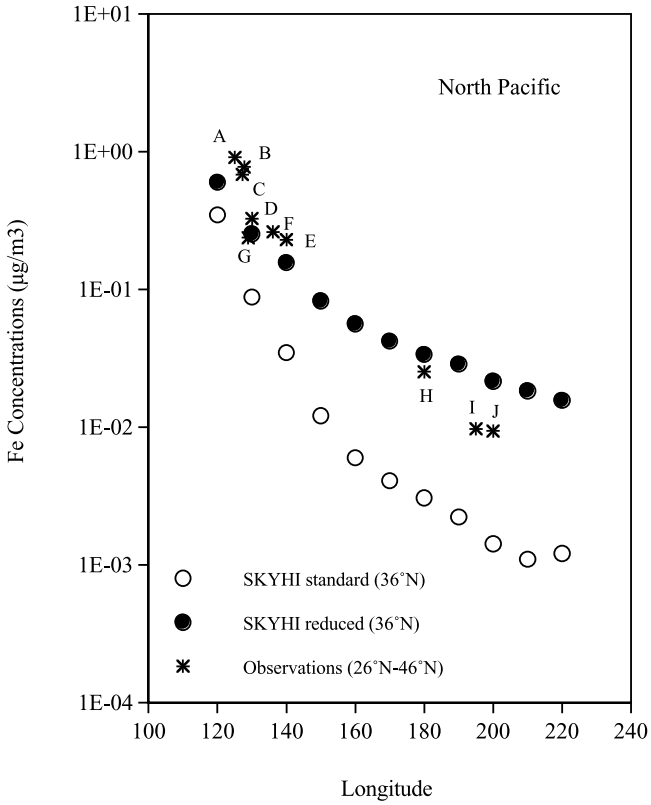

Figure 1. Longitudinal variation of the aeolian Fe concentrations from the Asian coast to the North Pacific simulated by SKYHI using two different precipitation thresholds for removal (standard threshold precipitation rate = 0.01 cm day^{-1}, open circles, and reduced threshold precipitation rate = 1 cm day^{-1}, filled circles). Observation locations from *Gao et al.* [2001] are: A. Qingdao (36°N, 126°E), B. Mallipo (37°N, 128°E), C. Cheju Island (33°N, 127°E), D. East China Sea (31°N, 130°E), E. Sapporo (43°N, 142°E), F. Wajima (37°N, 136°E), G. Onna (26°N, 128°E), H. Midway (28°N, 177°W), I. Northeast Pacific (26°N, 155°W), and J. Northeast Pacific (40°N, 165°W).

from aerosol particles less than 3 μm than from larger particles. Their studies highlight the potential impact of fine aerosol particles on delivery of aerosol Fe to the ocean surface.

[15] The concentrations of dust over different regions of the global ocean vary as a function of season, driven by seasonal variability of dust emissions, transport and wet removal. Figure 3 shows monthly mean dust concentrations (the silt fraction) in the bottom layer of SKYHI during January, April, July, and October based on the GISS source fields. Over the western N. Pacific, for example, the highest concentrations appear in the spring, due to high dust production in deserts in western and northern China and strong westerly transport occurring in that season [*Merrill*, 1989]. In the North Atlantic, the dust loading is strongly affected by the African source, particularly in the summer [*Prospero*, 1996b]. However, there are several large regions over the oceans where dust concentrations are low and vary little with season, including the equatorial Pacific and eastern South Pacific, known as high nitrate low chlorophyll (HNLC) regions, and Southern Ocean, to which the corresponding dust fluxes are well below 2 mg m^{-2} mon^{-1} (equivalent to an aeolian Fe deposition of 0.07 mg m^{-2} mon^{-1}). Thus the dust distributions predicted by the SKYHI model coincide with some of the Fe deficiency regions, in particular HNLC regions.

[16] The dust plume from Australia predicted by SKYHI simulations using the GISS emissions seem inconsistent with satellite AVHRR images, which do not have this dust plume feature [*Husar et al.*, 1997]. Dust activities in Australia have been well studied [*McTainsh et al.*, 1998; *McTainsh*, 1999]. Examination of clay mineral particles in Antarctic ice cores [*Gaudichet et al.*, 1992] and GCM model simulations in comparison with ice core and sediment records [*Mahowald et al.*, 1999] provide constraints on the contribution of Australian dust to the Antarctic during both Last Glacial Maximum and at present. Trajectory analyses suggest that the known red-snow events in the Southern Alps of New Zealand are due to dust transport from Australian sources. Therefore Australian dust certainly has regional impacts. However, our modeled dust concentrations near Australia appear to be too high in comparison to observations.

[17] One of the causes for disagreements in dust between model estimates and observations in Australia could be uncertainties associated with dust source identifications such as overestimating the contributions of desert sources to the total dust load in that region [*Tegen and Miller*, 1998]. High dust emissions are predicted in the models in the western part of the Australian continent instead of the Lake Eyre basin where most dust activities are observed in Australia [*McTainsh et al.*, 1998]. This closed inland drainage basin,

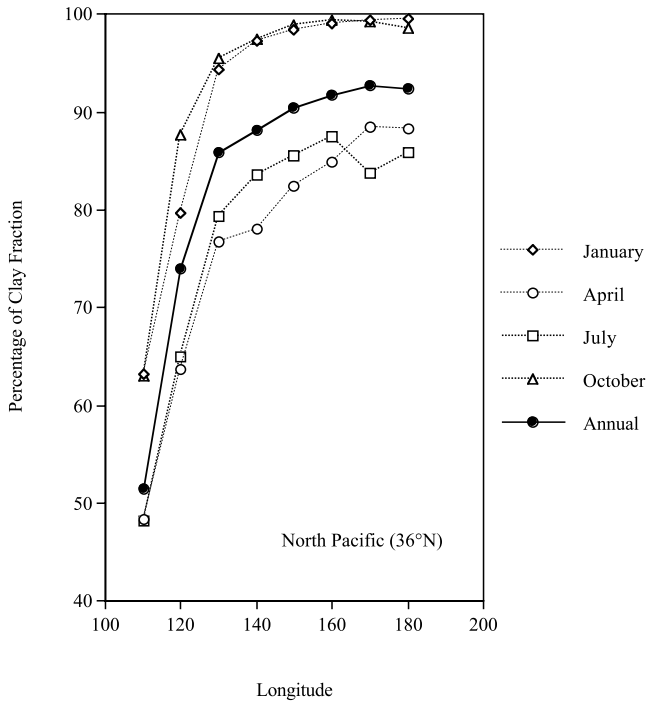

Figure 2. Variation of the clay fraction of dust mass from the GISS emissions as a function of distance from the Asian coast.

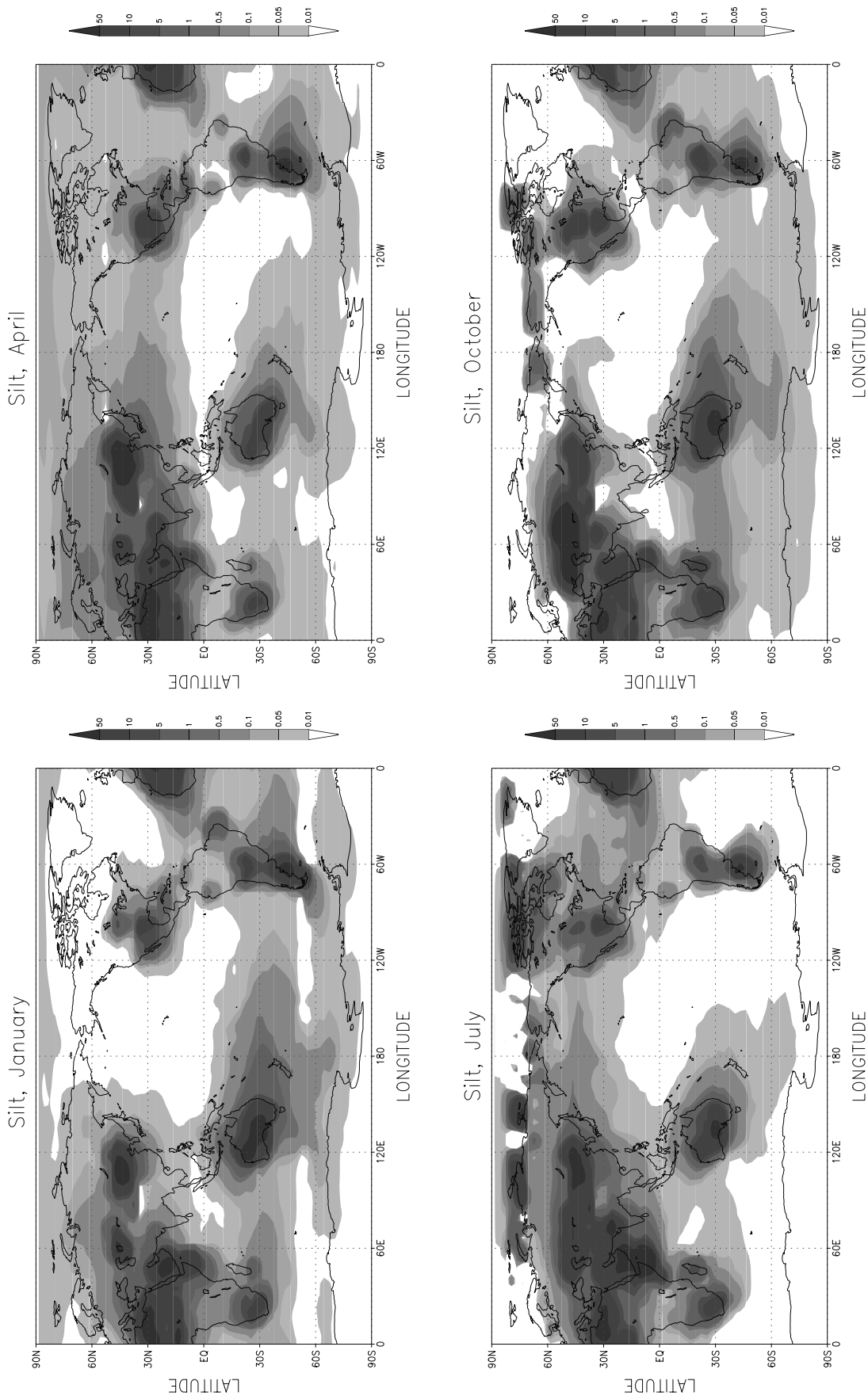

Figure 3. Simulated global distributions of dust (silt, 1–10 μm) in the surface layer, using the GISS emissions.

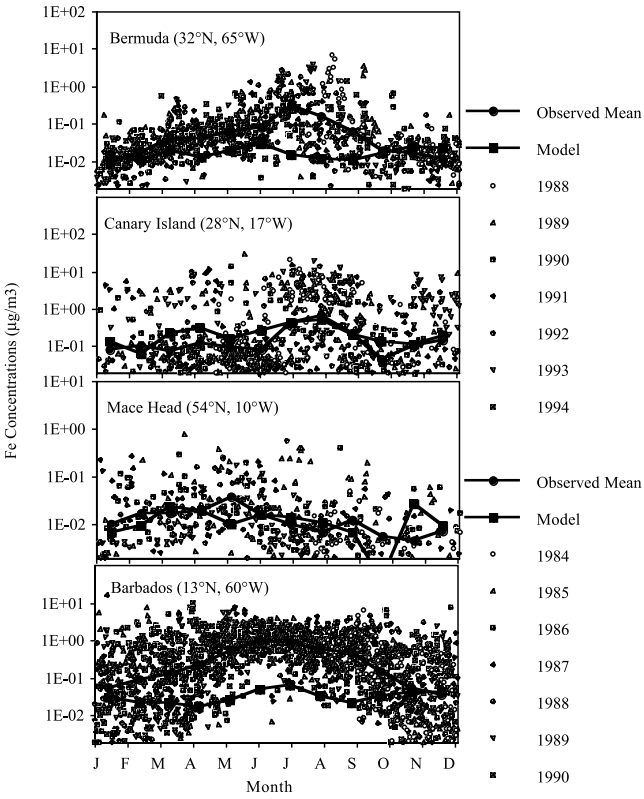

Figure 4a. Comparison of monthly Fe concentrations at four locations in the Atlantic between observations made in the marine boundary layer and the SKYHI model results using the GISS emissions.

with a total area of 1,140,000 km^2, is normally dry most of the year and experiences very low rainfall. The importance of this region as a dust source has been confirmed by TOMS observations [*Prospero et al.*, 2002]. Similar situations also occur in other regions. During a recent aerosol characterization experiment in the Asian-Pacific region, the consistency between modeled activities of dust and those from in situ measurements in east Asia was achieved after improvement of the dust source fields by considering the development of new dust sources in the region (M. Chin, personal communication, 2001). These results demonstrate the importance of obtaining accurate global dust source fields in order to improve model simulations.

[18] Figures 4a and 4b show comparisons between modeled and observed Fe concentrations at specific locations on a seasonal basis. In the Atlantic sector (Figure 4a), we selected four locations where multi-year, daily Fe concentrations were measured: Bermuda, Canary Island, Mace Head, and Barbados. In general, the modeled results follow the general distributions of the measurements, in particular the model and observation fits reasonably well for locations near dust sources, such as Canary Island, which is located right off the west coast of Africa. However, the model predicts lower than observed concentrations, in particular at Bermuda and Barbados. This may be due to an underestimated source strength in North Africa (see below). The model predicted Fe concentrations agree with observed values at four locations in the Pacific that were derived from Al measurements (Figure 4b). The comparison at Cheju Island does not look as good as the open ocean sites, suggesting that large concentration gradients near source regions make it difficult for the model to simulate for those locations exactly. Figure 4c shows a model-observation comparison of Fe concentrations on an annual basis at 27 locations (Table 2).

[19] To explore the possibility that the source strength may contribute to the underestimation of Fe concentrations in the Atlantic by the model, we compare the GISS and the GOCART sources by region (Figures 5a and 5b). The GISS emission rates are lower in North Africa and Asia but higher in Australia and North America (Figure 5a). The biases between the GISS and the GOCART sources appear to be present throughout the year (Figure 5b). This may partially explain why the modeled concentrations derived from the GISS source field are lower for the Atlantic region compared with measured concentrations.

4. Aeolian Iron Deposition Fluxes

4.1. Model Predictions and Measurement-Based Estimates of Deposition Fluxes

[20] In a recent paper, *Fung et al.* [2000] presented modeling results of aeolian Fe fluxes and an analysis of the Fe budget in the upper ocean. They focused on four regions with different dust input characteristics: the Equa-

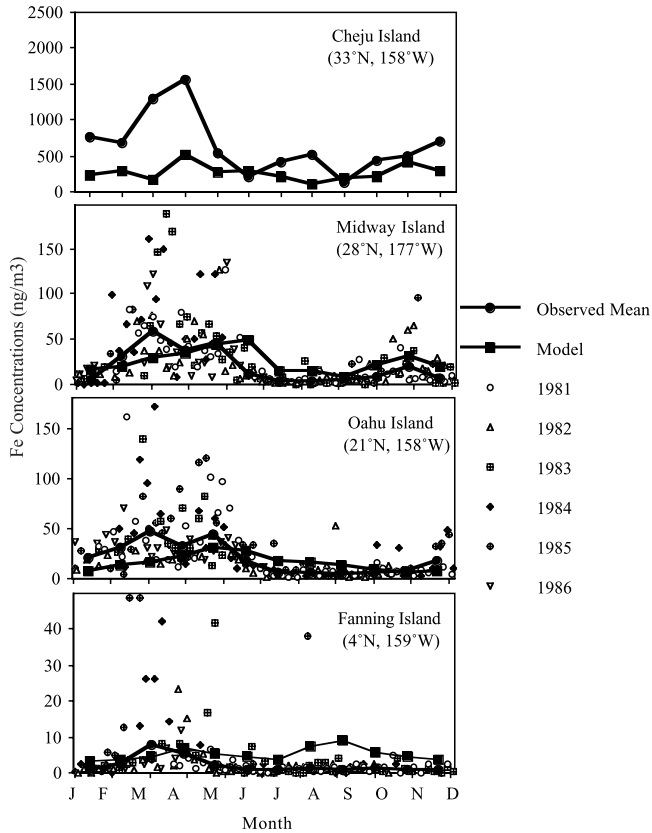

Figure 4b. Comparison of monthly Fe concentrations at four locations in the Pacific between observations made in the marine boundary layer and the SKYHI model results using the GISS emissions.

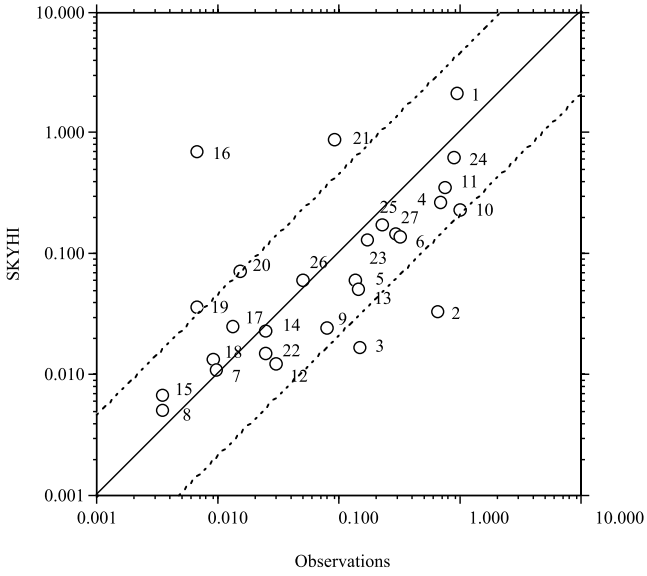

Figure 4c. Comparison of annual Fe concentrations at 27 locations between observations made in the marine boundary layer and the SKYHI model results using the GISS emissions. Solid line indicates 1:1 relation; dashed lines indicate 2-standard deviations.

torial Pacific, Southern Ocean, Northeast Pacific, and Northwest Pacific. Table 3 shows a comparison of our SKYHI model results with those of Fung et al. for these four regions. Deposition estimates based on dust measurements are also included in this table for comparison. The models agree with each other within a factor of two or three, as the same dust emission fields were used. The differences between the model simulations are due primarily to the different transport and treatment of rainout/washout processes in the models. The results from both models agree reasonably well with the observation-based flux estimates for the Equatorial Pacific, Southern Ocean, and Northwest Pacific sites. For the Northeast Pacific site, however, the model results are significantly higher than the fluxes estimated based on two weekly measurements, which were made on a research cruise during the period of May and June [*Zhuang et al.*, 1992a]. Data from that cruise indicate that the mass medium diameters (MMD) of dust particles vary dramatically under similar ambient conditions [*Arimoto et al.*, 1997]. These MMD variations could indicate substantial changes in dust concentrations. Considering dust concentration variations and their seasonal variability, shipboard measurements over a short period of time are not likely to be representative of the annual average. Table 3 also gives the relative contribution of wet deposition from the SKYHI model simulations (see discussion below).

Table 2. Locations for Model-Observation Comparison on Annual Fe Concentrations

Site No.	Name	Location	References
1	Arabian	Sea 20°N, 60°E	*Tindale and Pease* [1999]
2	Barbados	13°N, 60°W	*Arimoto et al.* [1995]
3	Bermuda	32°N, 65°W	*Arimoto et al.* [1995]
4	Cheju	33°N, 126°E	*Arimoto et al.* [1995]
5	Chichijima	27°, 142°E	*Tsunogai et al.* [1985]
6	East China Sea	31°N, 130°E	*Gao et al.* [1997]
7	Enewetak	11°N, 162°E	*Uematsu et al.* [1983]
8	Fanning Island	4°N, 159°W	*Uematsu et al.* [1983]
9	Guam	13°N, 145°E	*Uematsu et al.* [1983]
10	Izana	28°N, 17°W	*Arimoto et al.* [1995]
11	Mallipo	37°N, 128°E	*Gao et al.* [1997]
12	Mace Head	54°N, 10°W	*Arimoto et al.* [1995]
13	Miami	26°N, 80°W	*Prospero* [1999]
14	Midway	28°N, 177°W	*Uematsu et al.* [1983]
15	Nauru	1°S, 167°E	*Prospero et al.* [1989]
16	New Caledonia	21°S, 166°E	*Prospero et al.* [1989]
17	N.E. Pacific-1	40°N, 165°W	*Zhuang et al.* [1992a]
18	N.E. Pacific-2	26°N, 155°W	*Zhuang et al.* [1992a]
19	N. New Zealand	35°S, 173°E	*Arimoto et al.* [1997]
20	Norfolk	29°S, 167°E	*Prospero et al.* [1981]
21	New York Bight	40°N, 73°W	*Gao et al.* [2002]
22	Oahu	21°N, 158°W	*Uematsu et al.* [1983]
23	Okinawa	27°N, 128°E	*Tsunogai et al.* [1985]
24	Qingdao	36°N, 120°E	*Gao et al.* [1997]
25	Sapporo	43°N, 142°E	*Tsunogai et al.* [1985]
26	Shemya	53°N, 174°E	*Uematsu et al.* [1983]
27	Xiamen	24°N, 118°E	*Gao et al.* [1997]

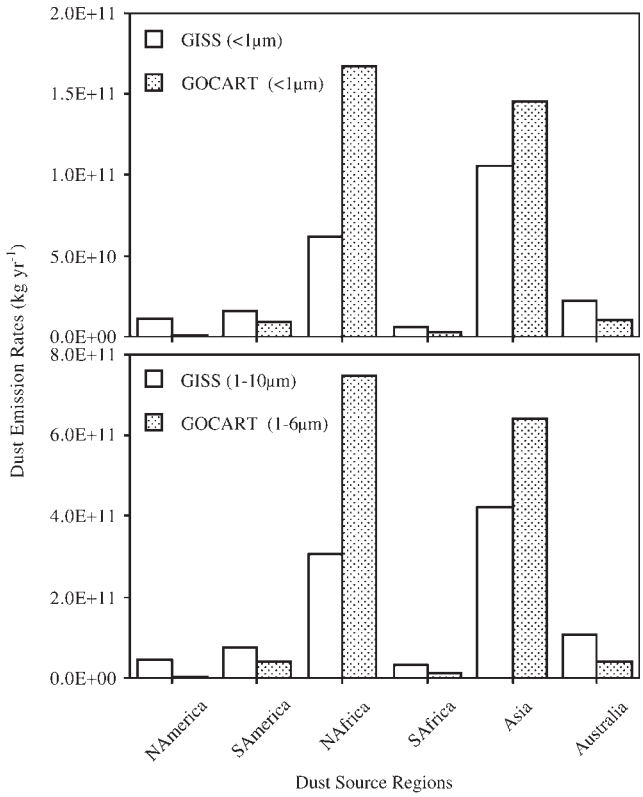

Figure 5a. Comparison of annual dust emission rates between GISS and GOCART for major source regions.

4.2. Relative Contribution of Wet Deposition to the Total Aeolian Iron Fluxes

[21] To examine the contribution of wet deposition to the total aeolian Fe fluxes, we calculate dry and wet deposition separately based on measurements made at 73 marine locations using a simple deposition model, and compare these fluxes to the SKYHI results at corresponding locations using the GISS source fields. We combine the modeled silt and clay components to obtain the total deposition, since the measurement data do not have size-separated results. We

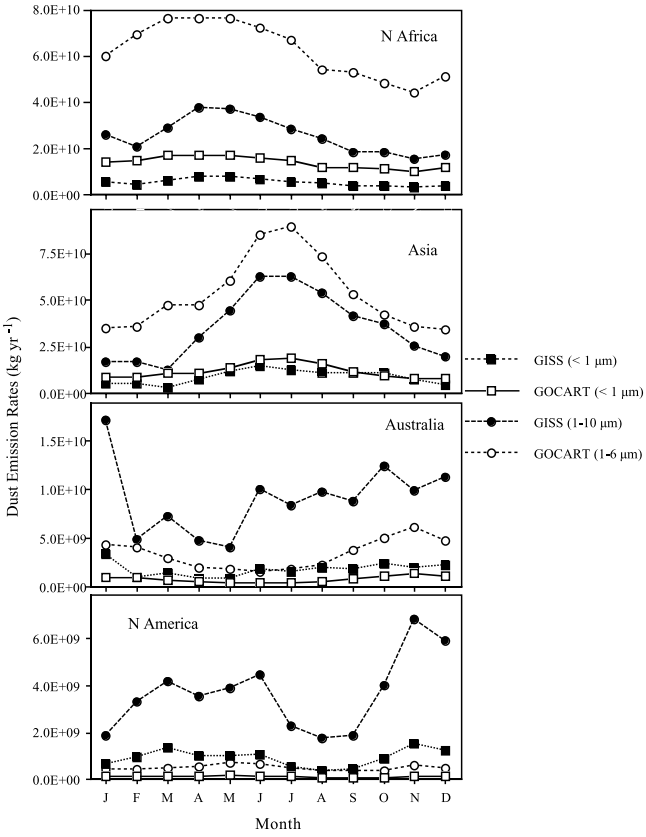

Figure 5b. Comparison of seasonal dust emission rates for major source regions between the field of *Tegen and Fung* [1994] and that of *Ginoux et al.* [2001].

also separate the coastal sites from the open ocean sites, based on the fact that there are significant differences in the concentration levels and in particle-size distributions between coastal oceans and open oceans. Figure 6 presents a comparison of the results. Both observations and model results suggest that aeolian Fe input by wet deposition accounts for an average of ~60% of the total deposition over open oceans. Over the coastal seas, the percentage of wet deposition decreases to ~40% on average. As a test of sensitivity, we compare the model results using the GOCART source field against both the model outputs using the GISS source field and observations at 19 specific locations, which were used for model-observation comparisons by *Ginoux et al.* [2001] and *Tegen and Fung* [1994].

Table 3. Comparison of Modeled and Measured Fe Fluxes (μmol m^{-2} yr^{-1})

Regions	Locations	SKYHI	*Fung et al.* [2000]	Measured[a]	SKYHI (%wet)
Eq. Pacific	0°, 140°W	2.7	6.5	1.8 (1)	53
S. Ocean	67°S, 110°W	2.3	1.0	4.3 (2)	32
N.E. Pacific	40°N, 160°W	32	56	(6.4) (3)	84
N.W. Pacific	40°N, 170°E	49	93	77 (4)	49

[a]*Fung et al.*, GBC, 2000.
[b]Fluxes were calculated based on measurements from the following locations: 0–12°S, 82–110°W [*Prospero and Bonatti*, 1969], 69°S, 76°E (Gao, Unpublished data), 40–47°N, 158–165°W [*Zhuang et al.*, 1992a], based on two weekly measurements made during May and June, 42°N, 139°E [*Uematsu et al.*, 1983]; 53°N, 174°E [*Tsunogai et al.*, 1985].

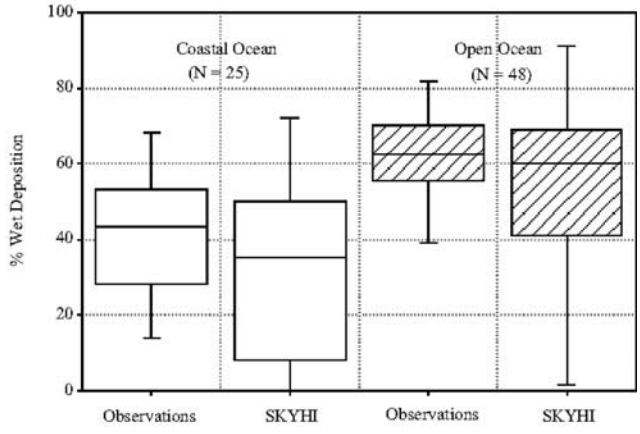

Figure 6. Relative contribution of wet deposition of Fe to the total deposition between coastal sea and open ocean derived from observations and model simulations using the GISS emissions.

Figures 7a and 7b indicate that all three sets of data and model results are consistent in suggesting the importance of wet deposition. The comparison thus suggests that this result is not sensitive to the different source fields. The result clearly demonstrates that precipitation scavenging is a major process in delivering aeolian Fe to the ocean on the global scale.

[22] The importance of wet deposition has been recognized at some marine locations. In the Pacific, the wet deposition of dust accounts for ~80% of the total deposition measured at a few locations [*Uematsu et al.*, 1985]. In the Mediterranean Sea, wet deposition of dust accounts for ~65–80% of the total dust deposition [*Molinaroli et al.*, 1993]. Although massive Saharan dust plumes are exported to the Mediterranean all year long, the periods during which dust fluxes to the ocean are high are associated with high precipitation rates, as observed at Corsica Island in the Mediterranean [*Bergametti et al.*, 1989]. Recent measurements on the bulk versus wet deposition fluxes at Bermuda by *Church et al.* [2000] and *Kim et al.* [1999] showed that wet deposition was the dominant process of the Fe input to the Sargasso Sea over most of their sampling seasons, with ~50% of the total Fe fluxes attributed to wet deposition on an annual basis. At Amsterdam Island, wet deposition is also significant, ranging from 35 to 43% of the total deposition [*Jickells and Spokes*, 2001]. These authors concluded that the temporal variation of dust deposition fluxes is related to the occurrence of precipitation, although the relationship between the total fluxes and the rainfall amounts is not linear. Similar results were also obtained at other locations, in particular the midlatitude areas [*Galloway et al.*, 1982]. The fact that Fe deposition fluxes are strongly affected by precipitation scavenging processes implies that the input of aeolian Fe to the ocean will be related to the concentrations of dust aloft as well as near the surface.

4.3. Dissolved Iron Fluxes and Natural Iron Fertilization in the Ocean

[23] Biological uptake of Fe largely depends on its solubility and chemical speciation in seawater [*Wells et*

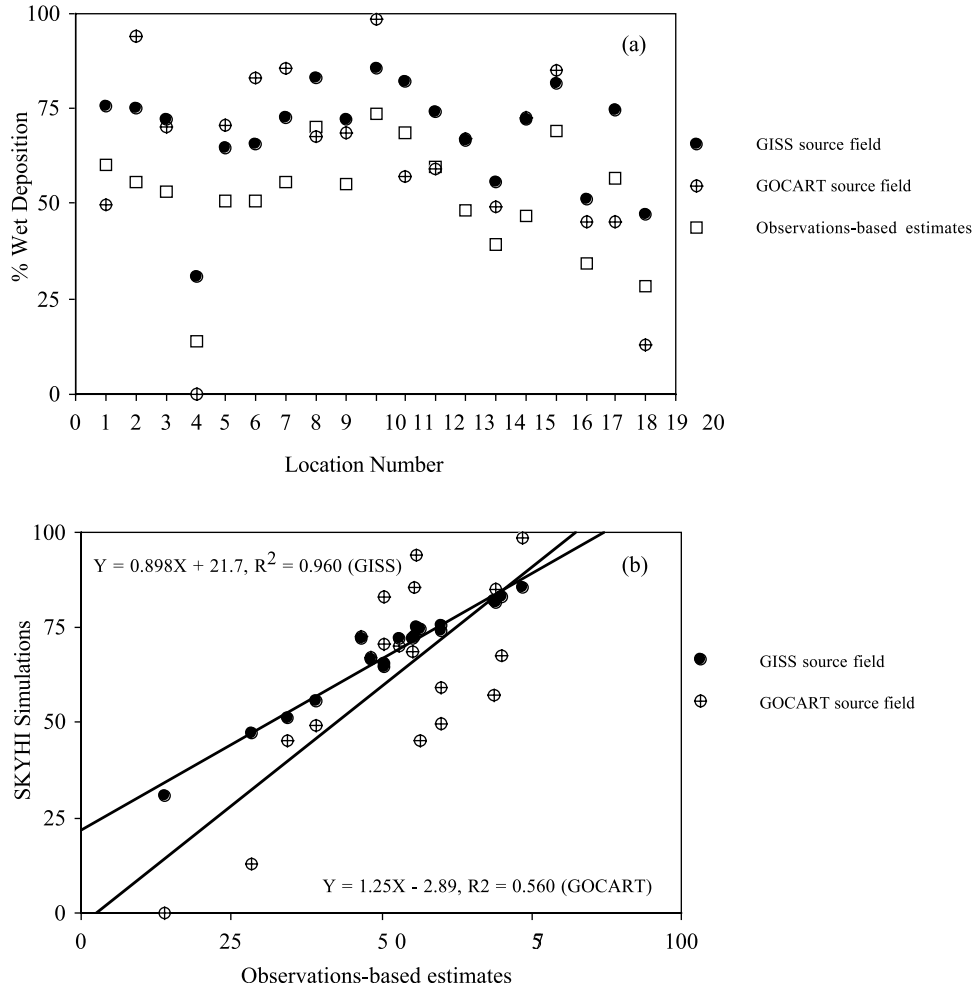

Figure 7. Relative contribution of wet deposition to the total deposition. (a) Comparison of model simulations using two different source fields (GISS field and GOCART field) with observations at 19 locations: 1. Barbados (13°N, 60°W), 2. Bermuda (32°N, 65°W), 3. Mace Head (54°N, 10°W), 4. Canary Island (28°N, 17°W), 5. Miami (26°N, 80°W), 6. Sandy Hook (40°N, 73°W), 7. Northeast Pacific (47°N, 158°W), 8. American Samoa (14°S, 171°W), 9. Norfolk (29°S, 167°E), 10. Funafuti (8°S, 179°E), 11. Okinawa (27°N, 128°E), 12. Shemya (53°N, 174°E), 13. Midway (28°N, 177°W), 14. Oahu (21°N, 158°W), 15. Enewetak (11°N, 162°E), 16. Fanning (4°N, 159°W), 17. Qingdao (36°N, 129°E), 18. Xiaman (24°N, 118°E), 19. Arabian Sea (15°N, 64°E). (b) Comparison of model simulations against observations at those 19 locations.

al., 1995]. Wet deposition through episodic precipitation events could be more efficient than chronic dry deposition in delivering nutrient elements to the ocean to promote biological responses such as those caused by nitrogen deposition observed in the open ocean [*Owens et al.*, 1992]. When dust particles encounter more acidic cloud droplets and become incorporated in precipitation, Fe in dust may undergo dissolution as the soluble ferrous iron [*Behra and Sigg*, 1990], which could increase bio-availability of aeolian Fe once deposited to the surface ocean. The solubility of Fe in precipitation has indeed been found to be a function of pH, although the relationship is not simple [*Colin et al.*, 1990; *Weschler et al.*, 1986]. In addition, photochemical reduction of Fe(III) involving $OH^{\cdot}$ radical in clouds, fog, and rain results in the formation of Fe(II), with the quantum efficiency for this photolysis reaction being as high as 0.14 ± 0.04 at 313 nm [*Faust and Zepp*, 1993; *Faust and Hoigne*, 1990]. This transformation of Fe(III) to Fe(II) could be enhanced during long-range transport, as suggested by *Zhuang et al.* [1992b] from their work in the North Pacific. These natural processes may significantly increase the amount of dissolved Fe in precipitation beyond the Fe solubility of a few percent directly measured from dust particles themselves [*Zhu et al.*, 1997; *Spokes and Jickells*, 1996]. *Zhuang et al.* [1995] determined the dissolved Fe (II) in rainwater collected over coastal Massachusetts and found that the total dissolved Fe (II) passing through a 0.4 μm pore size filter accounts for 25–53% of the total filterable Fe in rain waters. Recent volume-weighted measurements of rain collected in coastal North Carolina and filtered with 0.4 μm filters indicate that approximately half of the Fe in rainwater is dissolved [*Willey et al.*, 2000]. Estimates by *Jickells* [1999] indicate that the solubility of Fe in wet

Table 4a. Dissolved Fe in Precipitation Defined as Passing Through 0.4–0.45 μm Filters

Location	Date	# of Samples	Dissolved Fe, %	References
Brittany, France	Sep and Nov 1983	6	17	*Colin et al.* [1990]
Darmstadt, Germany	Feb 1989	2	50	*Hofmann et al.* [1991]
Massachusetts Bay	Jul 92–Jun 93	12	25–53[a]	*Zhuang et al.* [1995]
N.W. Mediterranean	1988–1989	45	11	*Guieu et al.* [1997]
Wilmington, NC, USA	Jul 1997–Jun 1999	112	50	*Willey et al.* [2000]
E. Mediterranean, Turkey	Feb 1996–Jun 1997	87	10	*Ozsoy and Saydam* [2001]

[a]Percentage of Fe (II) in the total dissolved Fe passing through 0.4 μm filters.

deposition to the Sargasso Sea is significantly higher than that in dry deposition. With the wet proportion accounting for half of the total Fe fluxes at Bermuda, *Church et al.* [2000] concluded that the total flux is more soluble than previously thought, and they suggest that an increased wet deposition of aeolian Fe may fuel an increase in nitrogen fixation in the region.

[24] To estimate a global budget of dissolved Fe delivery to the ocean, we applied our modeled proportion of wet deposition, that is, 40–60% of the total deposition, to the total aeolian Fe fluxes given by *Gao et al.* [2001], and then we applied a range of reported Fe solubility of 10–50% from precipitation measurements at a few locations as listed in Table 4a to obtain the dissolved aeolian Fe fluxes via wet deposition. In this calculation, we consider dissolved Fe in precipitation as that passing through 0.4–0.45 μm filters. To estimate dissolved Fe fluxes by dry deposition, we assumed a range of 1–6% as a dissolved Fe fraction in dust based on dust leaching experiments (Table 4b). As dissolved Fe concentration in leaching solutions increased dramatically with pH decrease [*Zhuang et al.*, 1992a], the percentages of dissolved Fe derived from these leaching experiments should be considered as upper limits, as the pH (1–2) used in most of these experiments are substantially lower than that of rainwater. The total dissolved Fe fluxes from both wet deposition and dry deposition are reported in Table 5. Our estimates suggest that the global deposition of dissolved Fe to the ocean via wet deposition ranges from 0.5 to 4×10^{12} g yr^{-1}, accounting for 4–30% of the total aeolian Fe fluxes (with a midpoint of 17%). On the other hand, dry deposition of soluble Fe accounts for only 0.6 to 2.4% of the total aeolian Fe deposition. The combined total deposition (wet + dry) of dissolved aeolian Fe ranges from 0.62 to 4.4×10^{12} g yr^{-1}, accounting for 4.6 to 32 % of the total deposition. By comparison, a contribution of 10% has been suggested as an upper limit for soluble Fe in aeolian deposition fluxes to the ocean [e.g., *Fung et al.*, 2000].

[25] We note that our estimates involve substantial uncertainties. In most cases, the dissolved Fe is operationally defined as that passing through 0.4 μm pore size filters. Dissolved Fe traditionally defined in this way has been found to contain truly soluble Fe and colloidal Fe in seawater [*Wu et al.*, 2001]. A portion of dissolved Fe in rain has also been observed to be in a colloidal form (0.4–0.1 μm) [*Hoffman et al.*, 1991]. In addition, a 50% Fe solubility in precipitation was observed over the coastal oceans, which may be affected by anthropogenic sources, and therefore this solubility must be viewed as an upper limit for the dissolved Fe in precipitation.

[26] Aeolian Fe wet deposition may partially explain the observed phytoplankton distribution in the surface ocean. During a sediment trap study conducted in the oligotrophic eastern Mediterranean (~34°N, 20°E), *Rutten et al.* [2000] observed a clear positive correlation between chlorophyll *a* concentrations in the surface waters and precipitation rates. These authors argued that high dust input could be attributed to high precipitation rates [*Molinaroli et al.*, 1993]. We reexamined this trend for several additional locations in the region using more recent SeaWiFS chlorophyll climatology and the precipitation climatology of *da Silva et al.* [1994], and we found that chlorophyll concentrations at these locations also co-vary with those of precipitation. Although other factors such as variations of mixed layer depth, nutrient supply, and lateral advection of continental substances may contribute to the observed chlorophyll distributions, the temporal chlorophyll-precipitation linkage in this region suggests that aeolian Fe input through precipitation washout could result in more Fe that can be readily used by marine organisms. Observations by *Young et al.* [1991] conducted in spring in the open North Pacific indicate that a significant increase (>60%) in primary production in surface seawaters is associated with high dust fluxes, but they did not separate wet deposition from the total deposition fluxes. We speculate that wet deposition is likely dominant under typical oceanic conditions.

[27] Results from these studies lead us to conclude that aeolian Fe input through precipitation scavenging may be

Table 4b. Percentage of Dissolved Iron in Dust Determined Through Leaching Experiments

Source of Sample	Fe (II),[a] %	Dissolved Fe,[b] %	pH	Reference
Chinese loess	<1			*Zhuang et al.* [1992b]
Saharan aerosol	1		2	*Spokes and Jickells* [1996]
Urban aerosol	8.4		2	*Spokes and Jickells* [1996]
Dust at Barbados	1.7	6.2	1	*Zhu et al.* [1997]
Arabian Sea	<4		4.2	*Siefert et al.* [1999]

[a]Soluble Fe (II) fraction.
[b]Total dissolved Fe fraction.

Table 5. Atmospheric Deposition of Dissolved Iron to the Major Ocean Basins (10^{12} g yr^{-1})

Ocean Basin	Total Deposition[a]	Wet Deposition of Dissolved Fe[b]	Dry Deposition of Dissolved Fe[c]	Total Deposition of Dissolved Fe
North Pacific	3.0	0.12–0.89	0.018–0.071	0.14–0.96
South Pacific	0.31	0.012–0.094	0.0019–0.0075	0.014–0.10
North Atlantic	6.6	0.26–1.9	0.039–0.16	0.30–2.1
South Atlantic	0.59	0.023–0.18	0.0035–0.014	0.027–0.19
Indian	2.4	0.096–0.72	0.014–0.058	0.11–0.78
Antarctic	0.071	0.0028–0.021	0.00043–0.0017	0.0032–0.023
Arctic	0.13	0.0051–0.038	0.00076–0.0030	0.0058–0.041
Mediterranean	0.54	0.022–0.16	0.0032–0.013	0.025–0.17
Global Total	14	0.54–4.1	0.081–0.32	0.62–4.4
% of the total deposition (lower-upper limits)		4–30	0.6–2.4	4.6–32

[a]Estimates of Fe deposition of *Gao et al.* [2001].
[b]Based on wet deposition accounting for 40–60% of the total deposition, and dissolved Fe in rain ranging 10–50% (Table 4a).
[c]Assuming dissolved Fe in dust accounting for 1–6% of the total aerosol Fe (Table 4b).

related to episodes of high surface ocean productivity at least in certain oceanic regions. Iron fertilization experiments have given strong support to the Fe limitation hypothesis [*Martin et al.*, 1994; *Coale et al.*, 1996b; *Boyd et al.*, 2000]. The supply of soluble aeolian Fe through wet deposition may cause natural iron fertilization events that could be used to understand the role of iron as a critical nutrient in oceanic biogeochemical cycles.

5. Conclusions

[28] The primary focus of this work has been to investigate the air-to-sea deposition processes that control aeolian iron delivery to the ocean. We used the GFDL SKYHI atmospheric transport model to simulate atmospheric transport and deposition processes. Our results show temporal and spatial variation of dust concentrations, consistent with oceanic observations of extremely low dust concentrations over the equatorial Pacific and Southern Ocean. Model simulations also demonstrate that large silt particles are removed rapidly near the dust sources, with small clay particles dominating dust concentration over the open ocean.

[29] Both model simulations and observations suggest that wet deposition through precipitation scavenging accounts for ~40% of the total air-to-sea deposition of aeolian Fe over the coastal sea and ~60% over the open ocean. Our estimates of the global deposition of dissolved Fe to the ocean indicate that the annual input of dissolved Fe by precipitation scavenging ranges from 0.5 to 4×10^{12} g yr^{-1}, accounting for 4–30% of the total aeolian Fe fluxes (with a midpoint of 17%). The input of dissolved aeolian Fe by dry deposition accounts for only 0.6–2.4% of the total Fe deposition. Our results suggest that the estimate of 10% for soluble aeolian Fe currently considered as an upper limit may be too low. This highlights the need to make measurements of dissolved Fe in rainwater over the oceans. The importance of precipitation scavenging in delivering aeolian Fe to the ocean shown in this work suggests that precipitation distributions may play a crucial role in delivering aeolian Fe to the ocean and causing an increased biological production in the ocean.

[30] **Acknowledgments.** We wish to thank I. Tegen and P. Ginoux for providing the dust source emission fields. We thank J. Yoder for providing SeaWiFS chlorophyll data. We thank R. A. Duce, R. Arimoto, and M. Uematsu for providing the seasonal aerosol data collected in the Pacific and Atlantic. Our appreciation also goes to A. Rurren and P. Ziveri for sharing their Mediterranean data with us. We thank P. Falkowski, V. Ramaswamy, J. Prospero, G. McTainsh, J. Gras, M. Chin, T. Church, and L. Donner for comments and discussions. The manuscript was significantly improved by constructive reviews from two anonymous reviewers. This work is sponsored by NASA EOS/IDS grant NAG 5-9340. We acknowledge additional support from Center for Environmental BioInorganic Chemistry (CEBIC) through NSF grant CHE9810248 and Carbon Modeling Consortium (CMC) through NOAA grant NA96GP0312, both at Princeton University.

References

Archer, D. E., and K. S. Johnson, A model of the iron cycle in the ocean, *Glob. Biogeochem. Cyc.*, *14*, 269–280, 2000.

Arimoto, R., R. A. Duce, B. J. Ray, J. D. Cullen, J. T. Merrill, and W. G. Ellis Jr., Trace elements in the atmosphere over the North Atlantic, *J. Geophys. Res.*, *100*, 1199–1213, 1995.

Arimoto, R., B. J. Ray, N. F. Lewis, U. Tomza, and R. A. Duce, Mass-particle size distributions of atmospheric dust and the dry deposition of dust to the remote ocean, *J. Geophys. Res.*, *102*, 15,867–15,874, 1997.

Arnold, E., J. Merrill, M. Leinen, and J. King, The effect of source area and atmospheric transport on mineral aerosol collected over the North Pacific Ocean, *Global Planet. Change*, *18*, 137–159, 1998.

Balkanski, Y. J., D. J. Jacob, G. M. Gardner, W. C. Graustein, and K. K. Turekian, Transport and residence times of tropospheric aerosols inferred from a global three-dimensional simulation of ^{210}Pb, *J. Geophys. Res.*, *98*, 20,573–20,586, 1993.

Behra, P., and L. Sigg, Evidence for redox cycling of iron in the atmospheric water droplets, *Nature*, *344*, 419–421, 1990.

Bergametti, G., L. Gomes, E. Remoudaki, M. Desbois, D. Martin, and P. Buat-Ménard, Present transport and deposition patterns of African dusts to the North-Western Mediterranean, in *Paleoclimatology and Paleometeorology: Modern and Past Patterns of Global Atmospheric Transport*, edited by M. Leinen and M. Sarnthein, NATO ASI Series, *282*, 227–252, 1989.

Boyd, P. W., et al., A mesoscale phytoplankton bloom in the polar Southern Ocean stimulated by iron fertilization, *Nature*, *407*, 695–702, 2000.

Broecker, W. S., and G. M. Henderson, The sequence of events surrounding termination II and their implications for the cause of glacial-interglacial CO_2 changes, *Paleoceanography*, *13*, 352–364, 1998.

Capone, D. G., J. P. Zehr, H. W. Paerl, B. Bergman, and E. J. Carpenter, Trichodesmium, a globally significant marine cyanobacterium, *Science*, *276*, 1221–1229, 1997.

Church, T., L. Alleman, A. Veron, and G. Kim, Long term and seasonal deposition of chrustal dust elements to the Sargasso Sea, *AGU Eos Trans.*, *81*, F70, 2000.

Claquin, T., M. Schulz, and Y. J. Balkanski, Modeling the mineralogy of atmospheric dust sources, *J. Geophys. Res.*, *104*, 22,243–22,256, 1999.

Coale, K. H., S. E. Fitzwater, R. M. Gordon, K. S. Johnson, and R. T. Barber, Control of community growth and export production by upwelled iron in the equatorial Pacific Ocean, *Nature*, *379*, 621–624, 1996a.

Coale, K. H., et al., A massive phytoplankton bloom induced by an ecosystem-scale iron fertilization experiment in the equatorial Pacific Ocean, *Nature*, *383*, 495–501, 1996b.

Colin, J. L., J. L. Jaffrezo, and J. M. Gros, Solubility of major species in precipitation: Factors of variation, *Atmos. Environ.*, *23*, 537–544, 1990.

Cooke, W. F., V. Ramaswamy, and P. Kasibhatla, A general circulation model study of the global carbonaceous aerosol distribution, *J. Geophys. Res.*, *107*(D16), 4279, doi:10.1029/2001JD001274, 2002.

Dana, M. T., and J. M. Hales, Statistical aspects of the washout of polydisperse aerosols, *Atmos. Environ.*, *10*, 45–50, 1976.

da Silva, A., A. C. Young, and S. Levitus, *Atlas of Surface Marine Data 1994*, NOAA Atlas NESDIS 6, U.S. Department of Commerce, Washington, D.C., 1994.

Dentener, F. J., G. R. Carmichael, Y. Zhang, J. Lelieveld, and P. J. Crutzen, Role of mineral aerosol as a reactive surface in the global troposphere, *J. Geophys. Res.*, *101*, 22,869–22,889, 1996.

Duce, R. A., and N. W. Tindale, Atmospheric transport of iron and its deposition in the ocean, *Limnol. Oceanogr.*, *36*, 1715–1726, 1991.

Falkowski, P. G., Evolution of the nitrogen cycle and its influence on the biological sequestration of CO_2 in the ocean, *Nature*, *387*, 272–275, 1997.

Faust, B. C., and J. Hoigne, Photolysis of Fe(III)-hydroxy complexes as sources of OH radicals in cloud, fog and rain, *Atmos. Environ.*, *24*, 79–89, 1990.

Faust, B. C., and R. G. Zepp, Photochemistry of aqueous Fe(III)-polycarboxylate complexes: Roles in the chemistry of atmospheric and surface waters, *Environ. Sci. Technol.*, *27*, 2517–2552, 1993.

Fung, I., S. K. Meyn, I. Tegen, S. C. Doney, J. G. John, and J. K. B. Bishop, Iron supply and demand in the upper ocean, *Glob. Biogeochem. Cyc.*, *14*, 281–295, 2000.

Galloway, J. N., J. D. Thornton, S. A. Norton, H. L. Volcjok, and R. A. MacLean, Trace metals in atmospheric deposition: A review and assessment, *Atmos. Environ.*, *16*, 1677–1700, 1982.

Gao, Y., R. Arimoto, R. A. Duce, X. Y. Zhang, G. Y. Zhang, Z. S. An, L. Q. Chen, M. Y. Zhou, and D. Y. Gu, Temporal and spatial distributions of dust and its deposition to the China Sea, *Tellus*, *49B*, 172–189, 1997.

Gao, Y., Y. J. Kaufman, D. Tanré, D. Kolber, and P. G. Falkowski, Seasonal distributions of aeolian iron fluxes to the global ocean, *Geophys. Res. Lett.*, *1*, 29–32, 2001.

Gao, Y., E. D. Nelson, M. P. Field, Q. Ding, H. Li, R. M. Sherrell, C. L. Gigliotti, D. A. Van Ry, T. R. Glenn, and S. J. Eisenreich, Characterization of atmospheric trace elements on PM2.5 particulate matter over the New York-New Jersey harbor estuary, *Atmos. Environ.*, *36*, 1077–1086, 2002.

Gaudichet, A., M. De Angelis, S. Joussaume, J. R. Petit, Y. S. Korotkevitch, and V. N. Petrov, Comments on the origin of dust in east Antarctica for present and ice-age conditions, *J. Atmos. Chem.*, *14*, 129–142, 1992.

Genthon, C., Simulations of desert dust and sea salt aerosols in Antarctica with a general circulation model of the atmosphere, *Tellus*, *44*, 371–389, 1992.

Ginoux, P., M. Chin, I. Tegen, J. M. Prospero, B. Holben, O. Dubovik, and S.-J. Lin, Sources and distributions of dust aerosols simulated with the GOCART model, *J. Geophys. Res.*, *106*, 20,255–20,273, 2001.

Giorgi, F., and W. L. Chameides, Rainout lifetimes of highly soluble aerosols and gases as inferred from simulations with a general circulation model, *J. Geophys. Res.*, *91*, 14,367–14,376, 1986.

GSS, Preparation of Geochemical Standard Reference Samples, *Natl. Bureau of Chem. Exploration Anal.*, Beijing, 1984.

Guieu, C., R. Chester, M. Nimmo, J.-M. Martin, S. Guerzoni, E. Nicolas, J. Mateu, and S. Keyes, Atmospheric input of dissolved and particulate metals to the northwestern Mediterranean, *Deep Sea Res.*, *44*, 655–674, 1997.

Hamilton, K., R. J. Wilson, J. D. Mahlman, and L. J. Umscheid, Climatology of the SKYHI troposphere-stratosphere-mesosphere general circulation model, *J. Atmos. Sci.*, *52*, 5–23, 1995.

Hicks, B. B., D. D. Baldocchi, T. P. Meyers, R. P. Hosker Jr., and D. R. Matt, A preliminary multiple resistance routine for deriving dry deposition velocities from measured quantities, Water, Air, and Soil Pollution, *36*, 311–330, 1987.

Hoffmann, H., P. Hoffmann, and K. H. Lieser, Transition metals in atmospheric aqueous samples, analytical determination and speciation, *Fresenius J. Anal. Chem.*, *340*, 591–597, 1991.

Holtslag, A. A. M., and B. A. Boville, Local versus nonlocalboundary-layer diffusion in a global climate model, *J. Climate*, *6*, 1825–1842, 1993.

Husar, R. B., J. M. Prospero, and L. L. Stowe, Characterization of tropospheric aerosols over the oceans with the NOAA advanced very high resolution radiometer optical thickness operational product, *J. Geophys. Res.*, *102*, 16,889–16,909, 1997.

Jickells, T. D., The input of dust derived elements to the Sargasso Sea: A synthesis, *Mar. Chem.*, *68*, 5–14, 1999.

Jickells, T. D., and L. J. Spokes, Atmospheric iron inputs to the ocean, in *Biogeochemistry of Iron in Seawater*, edited by D. Turner and K. A. Hunter, pp. 85–121, John Wiley, New York, 2001.

Kim, G., L. Y. Alleman, and T. M. Church, Atmospheric depositional fluxes of trace elements, 210Pb and 7Be to the Sargasso Sea, *Glob. Biogeochem. Cyc.*, *13*, 1183–1192, 1999.

Levy, H., II, and W. J. Moxim, Fate of US and Canadian combustion nitrogen emissions, *Nature*, *328*, 414–416, 1987.

Mahlman, J. D., and W. J. Moxim, Tracer simulation using a global general circulation model: Results from a mid-latitude instaneous source experiment, *J. Atmos. Sci.*, *35*, 1340–1374, 1978.

Mahlman, J. D., J. P. Pinto, and L. J. Umscheid, Transport, radiative, and dynamical effects of the Antarcticozone hole: A GFDL "SKYHI" model experiment, *J. Atmos. Sci.*, *51*, 489–508, 1994.

Mahowald, N., K. Kohfeld, M. Hansson, Y. Balkanski, S. P. Harrison, T. C. Prentice, M. Schulz, and H. Rodhe, Dust source and deposition during the last glacial maximum and current climate: A Comparison of model results with paleodata from ice cores and marine sediments, *J. Geophys. Res.*, *104*, 15,895–15,916, 1999.

Martin, J. H., Glacial-interglacial CO2 change: The iron hypothesis, *Paleoceanography*, *5*, 1–13, 1990.

Martin, J. H., et al., Testing the iron hypothesis in ecosystems of the equatorial Pacific ocean, *Nature*, *371*, 123–129, 1994.

McTainsh, G. H., Dust transport and deposition, in *Aeolian Environments, Sediments and Landforms*, edited by A. S. Goudie, I. Livingstone, and S. Stokes, pp. 191–211, John Wiley, New York, 1999.

McTainsh, G. H., A. W. Lynch, and E. K. Tews, Climate controls upon dust storm occurrence in eastern Australia, *J. Arid Environ.*, *39*, 457–466, 1998.

Merrill, J. T., Atmospheric long-range transport to the Pacific Ocean, in *Chemical Oceanography*, vol. 10, edited by J. P Riley, R. Chester, and R. A. Duce, pp. 15–50, Academic, New York,, 1989.

Molinaroli, E., S. Guerzoni, and G. Rampazzo, Contribution of Saharan dust to the central Mediterranean basin, *Geol. Soc. Am. Spec. Pap*, *284*, 303–312, 1993.

Owens, N. J. P., J. N. Galloway, and R. A. Duce, Episodic atmospheric nitrogen deposition to oligotrophic oceans, *Nature*, *357*, 397–399, 1992.

Ozsoy, T., and A. C. Saydam, Iron speciation in precipitation in the North-Eastern Mediterranean and its relationship with Sahara dust, *J. Atmos. Chem.*, *40*, 41–76, 2001.

Perry, K. D., and T. A. Cahill, Long-range transport of anthropogenic aerosols to the National Oceanic and Atmospheric Administration baseline station at Mauna Loa Observatory, Hawaii, *J. Geophys. Res.*, *104*, 18,521–18,533, 1999.

Petit, J. R., et al., Climate and atmospheric history of the past 420,000 years from the Vostok ice core, Antarctica, *Nature*, *399*, 429–436, 1999.

Prospero, J. M., Saharan dust transport over the North Atlantic Ocean and Mediterranean: An overview, in *The Impact of Desert Dust across the Mediterranean*, edited by S. Guerzoni and R. Chester, 404 pp., Kluwer Acad., Norwell, Mass., 1996a.

Prospero, J. M., The atmospheric transport of particles to the ocean, in *Particle Flux in the Ocean*, edited by V. Ittekkot et al., pp. 19–52, John Wiley, New York, 1996b.

Prospero, J. M., Long-term measurements of transport of African mineral dust to the Southeastern United States: Implications for regional air quality, *J. Geophys. Res.*, *104*, 15,917–15,927, 1999.

Prospero, J. M., and E. Bonatti, Continental dust in the atmosphere of the eastern equatorial Pacific, *J. Geophys. Res.*, *74*, 3362–3371, 1969.

Prospero, J. M., R. A. Glaccum, and R. T. Nees, Atmospheric transport of soil dust from Africa to South America, *Nature*, *289*, 570–572, 1981.

Prospero, J. M., M. Uematsu, and D. L. Savoie, Mineral aerosol transport to the Pacific Ocean, in *Chemical Oceanography*, vol. 10, edited by J. P. Riley, R. Chester, and R. A. Duce, pp. 188–218, Academic, San Diego, Calif., 1989.

Prospero, J. M., P. Ginoux, O. Torres, and S. E. Nicholson, Environmental characterization of global sources of atmospheric soil dust identified with the Nimbus 7 Total Ozone Mapping Spectrometer (TOMS) absorbing aerosol product, *Rev. Geophys.*, *40*(1), 1002, doi:10.1029/2000RG000095, 2002.

Rea, D. K., and S. A. Hovan, Grain size distribution and depositional processes of the mineral component of abyssal sediments: Lessons from the North Pacific, *Paleoceanography*, *10*, 251–258, 1995.

Rutten, A., G. J. de Lange, P. Ziveri, J. Thomson, P. J. M. van Santvoort, S. Colley, and C. Corselli, *Palaeogeography, Palaeoclimatology, Palaeoecology*, *158*, 197–213, 2000.

Siefert, R. L., A. M. Johansen, and M. R. Hoffmann, Chemical characterization of ambient aerosol collected during the southwest monsoon and intermonsoon seasons over the Arabian Sea: Labile-Fe(II) and other trace metals, *J. Geophys. Res.*, *104*, 3511–3526, 1999.

Sokolik, I. N., and O. B. Toon, Incorporation of mineralogical composition into models of the radiative properties of mineral aerosol from UV to IR wavelengths, *J. Geophys. Res.*, *104*, 9423–9444, 1999.

Spokes, L. J., and T. D. Jickells, Factors controlling the solubility of aerosol trace metals in the atmosphere and on mixing into seawater, *Aquatic Geochem.*, *1*, 355–374, 1996.

Sunda, W. G., Bioavailability and bioaccumulation of iron in the sea, in *The Biogeochemistry of Iron in Sea Water*, edited by K. A. Hunter and D. R. Turner, pp. 41–84, John Wiley, New York, 2001.

Taylor, S. R., and S. M. McLennan, *The Continental Crust: Its Composition and Evolution*, 312 pp., Blackwell Scientific, 1985.

Tegen, I., and I. Fung, Modeling of mineral dust in the atmosphere: Sources, transport and optical thickness, *J. Geophys. Res.*, *99*, 22,897–22,914, 1994.

Tegen, I., and R. Miller, A general circulation model study on the interannual variability of soil dust aerosol, *J. Geophys. Res.*, *103*, 25,975–25,995, 1998.

Tindale, N. W., and P. P. Pease, Aerosols over the Arabian Sea: Atmospheric transport pathways and concentrations of dust and sea salt, *Deep Sea Res., Part II*, *46*, 1577–1595, 1999.

Tsunogai, S., T. Suzuki, T. Kurata, and M. Uematsu, Seasonal and areal variation of continental aerosol in the surface air over the western North Pacific, *J. Oceanogr. Soc. Japan*, *41*, 427–434, 1985.

Uematsu, M., R. A. Duce, J. M. Prospero, L. Chen, J. T. Merrill, and J. T. Mc Donald, Transport of mineral aerosol from Asia over the Pacific Ocean, *J. Geophys. Res.*, *88*, 5345–5352, 1983.

Uematsu, M., R. A. Duce, and J. M. Prospero, Deposition of atmospheric mineral particles in the North Pacific Ocean, *J. Atmos. Chem.*, *3*, 123–138, 1985.

Underwood, G. M., C. H. Song, M. Phadnis, G. R. Carmichael, and V. H. Grassian, Heterogeneous reactions of NO2 and HNO3 on oxides and mineral dust: A combined laboratory and modeling study, *J. Geophys. Res.*, *106*, 18,055–18,066, 2001.

Watson, A. J., and N. Lefevre, The sensitivity of atmospheric CO_2 concentrations to input of iron to the oceans, *Tellus*, *51B*(2), 453–460, 1999.

Wells, M. L., N. M. Price, and K. W. Bruland, Iron chemistry in seawater and its relationship to phytoplankton: A workshop report, *Mar. Chem.*, *48*, 157–182, 1995.

Weschler, C. J., M. L. Mandich, and T. E. Graedel, Speciation, photosensitivity, and reaction of transition metal ions in atmospheric droplets, *J. Geophys. Res.*, *91*, 5189–5204, 1986.

Willey, J. D., R. J. Kieber, K. H. Williams, J. S. Crozier, S. A. Skrabal, and G. B. Avery Jr., Temporal variability of iron speciation in coastal rainwater, *J. Atmos. Chem.*, *37*, 185–205, 2000.

Wu, J., E. Boyle, W. Sunda, and L.-S. Wen, Soluble and colloidal iron in the oligotrophic North Atlantic and North Pacific, *Science*, *293*, 847–849, 2001.

Young, R. W., K. L. Carder, P. R. Betzer, D. K. Costello, R. A. Duce, G. R. DiTullio, N. W. Tindale, E. A. Laws, M. Uematsu, J. T. Merrill, and R. A. Feely, Atmospheric iron inputs and primary productivity: Phytoplankton responses in the north Pacific, *Glob. Biogeochem. Cyc.*, *5*, 119–134, 1991.

Zhu, X. R., J. M. Prospero, and F. J. Millero, Diel variability of soluble Fe(II) and soluble total Fe in North African dust in the trade winds at Barbados, *J. Geophys. Res.*, *102*, 21,297–21,305, 1997.

Zhuang, G., Z. Yi, R. A. Duce, and P. R. Brown, Chemistry of iron in marine aerosols, *Glob. Biogeochem. Cyc.*, *6*, 161–173, 1992a.

Zhuang, G., Y. Zhen, R. A. Duce, and P. R. Brown, Link between iron and sulphur cycles suggested by detection of Fe(II) in remote marine aerosols, *Nature*, *355*, 537–539, 1992b.

Zhuang, G., Z. Yi, and G. T. Wallace, Iron (II) in rainwater, snow, and surface seawater from a coastal environment, *Mar. Chem.*, *50*, 41–50, 1995.

S.-M. Fan, Y. Gao, and J. L. Sarmiento, Atmospheric and Oceanic Sciences Program, Princeton University, P. O. Box CN710, Sayre Hall, Princeton, NJ, USA. (fan@splash.princeton.edu; yuangao@splash.princeton.edu; jls@splash.princeton.edu)